European Radiology (2019) 29:5577–5589
https://doi.org/10.1007/s00330-019-06164-1

NEURO

Deteriorated functional and structural brain networks and normally appearing functional–structural coupling in diabetic kidney disease: a graph theory-based magnetic resonance imaging study

Yun Fei Wang[1] · Ping Gu[2] · Jiong Zhang[3] · Rongfeng Qi[1] · Michael de Veer[4] · Gang Zheng[1,4] · Qiang Xu[1] · Ya Liu[1] · Guang Ming Lu[1] · Long Jiang Zhang[1]

Received: 11 October 2018 / Revised: 18 February 2019 / Accepted: 14 March 2019 / Published online: 1 April 2019

Abstract

Purpose This study was conducted in order to investigate the topological organization of functional and structural brain networks in diabetic kidney disease (DKD) and its potential clinical relevance.

Methods Two hundred two subjects (62 DKD patients, 60 diabetes mellitus [DM] patients, and 80 healthy controls) underwent laboratory examination, neuropsychological test, and magnetic resonance imaging (MRI). Large-scale functional and structural brain networks were constructed and graph theoretical network analyses were performed. The effect of renal function on brain functional and structural networks in DKD patients was further evaluated. Correlations were performed between network properties and neuropsychological scores and clinical variables.

Results Progressing deteriorated global and local network topology organizations (especially for functional network) were observed for DKD patients compared with control subjects (all $p < 0.05$, Bonferroni-corrected), with intermediate values for the patients with DM. DKD patients showed normally appearing functional–structural coupling compared with controls, while DM patients manifested functional–structural decoupling ($p < 0.05$, Bonferroni-corrected). Impaired kidney function markedly affected functional and structural network organization in DKD patients (all $p < 0.05$). Urea nitrogen correlated with global and local efficiency in the structural networks ($r = -0.551$, $p < 0.001$; $r = -0.476$, $p < 0.001$, respectively). Global and local efficiency in the structural networks and normalized characteristic path length in the functional networks were associated with information processing speed and/or psychomotor speed.

Conclusion DKD patients showed enhanced functional and structural brain network disruption and normally appearing functional–structural coupling compared with DM patients, which correlated with kidney function, renal toxins, and cognitive performance.

Key Points

- *DKD patients showed markedly disrupted functional and structural brain network efficiency measures compared with DM patients and healthy controls.*
- *Reduced kidney function clearly deteriorated functional and structural brain networks in DKD patients.*
- *DKD patients displayed normally appearing functional–structural coupling compared with DM patients.*

Drs. Yun Fei Wang, Ping Gu had equal contributions to this work.

Electronic supplementary material The online version of this article (https://doi.org/10.1007/s00330-019-06164-1) contains supplementary material, which is available to authorized users.

✉ Long Jiang Zhang
kevinzhlj@163.com

Jiong Zhang
jiongzhang@live.com

[1] Department of Medical Imaging, Jinling Hospital, Medical School of Nanjing University, Nanjing 210002, Jiangsu, China

[2] Department of Endocrinology, Jinling Hospital, Medical School of Nanjing University, Nanjing 210002, China

[3] National Clinical Research Center of Kidney Disease, Jinling Hospital, Medical School of Nanjing University, Nanjing 210002, China

[4] Monash Biomedical Imaging, Monash University, Clayton, VIC 3168, Australia

Keywords Diabetic nephropathies · Diabetes mellitus · Diffusion tensor imaging · Magnetic resonance imaging

Abbreviations

γ	Normalized clustering coefficient
λ	Normalized characteristic path length
σ	Small-worldness
AAL	Automated anatomical labeling
ADA	American Diabetes Association
ANCOVA	Analysis of covariance
BUN	Blood urea nitrogen
Cp	Clustering coefficient
Cyst C	Cystatin C
DKD	Diabetic kidney disease
DM	Diabetes mellitus
DPARSF	Data Processing Assistant for Resting-State fMRI
DS	Deep subcortical
DTI	Diffusion tensor imaging
Eg	Global efficiency
eGFR	Estimated glomerular filtration rate
Eloc	Local efficiency
FBG	Fasting blood glucose
HbA1c	Hemoglobin A1c
HDL-C	High-density lipoprotein cholesterol
LDL-C	Low-density lipoprotein cholesterol
Lp	Characteristic path length
LTT	Line Tracing Test
MMSE	Mini-Mental State Examination
MoCA	Montreal Cognitive Assessment
MRI	Magnetic resonance imaging
NCT-A	Number Connection Test type-A
PV	Periventricular
rs-fMRI	Resting-state functional magnetic resonance imaging
SAS	Self-Rating Anxiety Scale
Scr	Serum creatinine
SDS	Self-Rating Depression Scale
SDT	Serial Dotting Test
TC	Total cholesterol
TIV	Total intracranial volume
Tri	Triglycerides
UA	Uric acid
WML	White matter lesions

Introduction

Type 2 diabetes has become a global pandemic [1–3]. Thanks to the development of anti-diabetes drugs and the use of insulin, the rates of diabetes-related complications have declined substantially in the past two decades [4]. However, despite these advances, the prevalence of diabetic kidney disease (DKD) is rising worldwide, which means that more and more DM patients are living with kidney complications [5, 6]. Type 2 diabetes-related cognition dysfunction has attracted more attention and has been studied in-depth in recent years [7, 8]. However, whether cognition impairments will progress in DKD patients and the underlying neural mechanism remain to be elucidated.

Neuroimaging provides a noninvasive and promising tool to uncover the neural basis of cognitive impairments in various diseases. However, to the best of our knowledge, only two studies by Sink et al [9] and Murea et al [10] explored brain microstructural changes in DKD individuals and their correlations with cognitive function scores and found that reduced kidney function had an adverse effect on brain volume and cognitive function. There is an urgent need to explore the neural mechanisms underlying cognitive dysfunction in DKD patients from the perspective of large-scale brain networks. There is increasing evidence suggesting that the human brain can be characterized as a large-scale integrated functional and structural network [11, 12]. The graph-based network approach has provided valuable insights into not only the architecture of whole-brain networks [13] but also the potential mechanisms underlying various cognitive deficits [14]. Using this approach, previous studies have characterized the topological properties of brain networks in the context of health and disease conditions [15–18]. Among numerous neuroimaging modalities, resting-state functional magnetic resonance imaging (rs-fMRI) and diffusion tensor imaging (DTI) are two promising tools to map intrinsic functional and structural brain networks in the human brain. Combining these two techniques could offer novel insights into the reconfiguration of neural network responses to various neuropsychology disorders. Finally, integrating the information from structural and functional networks could result in better understanding of brain changes in DKD patients.

We hypothesize that DKD patients showed more disrupted functional and structural brain network organization than those without kidney complication and the brain network alterations may be the neural mechanisms underlying cognitive dysfunction. For testing our hypothesis, we systemically investigated the large-scale functional and structural brain network alteration patterns in DKD patients compared with diabetes patients and healthy controls and explored the underlying neural mechanisms underlying cognitive dysfunction in DKD patients.

Materials and methods

Subjects

This prospective study was approved by the local Medical Research Ethics Committee. All participants gave written

informed consent. A total of 210 right-handed individuals participated in this study from April 2015 to August 2017, comprising 130 patients with type 2 diabetes and 80 age-, sex-, and education level-matched healthy controls (HCs). All HCs were recruited from the local community. The DM status was confirmed according to the diagnostic criteria published by the American Diabetes Association (ADA) [19]. Of all type 2 diabetes patients, 65 patients were clinically diagnosed as DKD according to the NKF–KDOQI™ guidelines [20]. Thus, all patients were further classified into two groups: DM group without kidney complication (DM group, $n = 65$) and the DKD group ($n = 65$). The inclusion criteria for HCs are as follows: (1) right handed, (2) age ≥ 18 years old, (3) could finish MR examination and cognitive assessments, (4) normal eyesight, (5) absence of any psychiatric or neurologic diseases, and (6) absence of medical illness impairing cognitive function. Exclusion criteria are (1) type 1 diabetes, diabetic ketoacidosis, or reported episodes of severe hypoglycemia; (2) previous history of neurological or psychiatric disease such as cerebral vascular disease, brain tumors, head trauma, epilepsy, Alzheimer's disease, or other dementia; (3) alcohol addiction or drug abuse history; and (4) contraindication of MR examination. Three DKD patients and three DM patients were excluded due to head-motion artifacts on structural and/or functional MR images. Two DM patients were ruled out owing to incomplete coverage of the whole brain during the MR examination. Thus, 62 DKD patients, 60 DM patients, and 80 HCs were included in the final analysis. Table 1 illustrates the demographic data of all 202 subjects.

Neuropsychological assessments

All participants underwent a battery of standardized cognitive assessments before MRI examinations. Global cognitive function was measured by the Mini-Mental State Examination (MMSE) and Montreal Cognitive Assessment Scale (MoCA). Memory function was assessed by the immediate and delayed recall Verbal Word Learning Test. Information processing speed was derived from the Stroop Color Word Test (Part I and II) and the Digit Symbol Test (DST) [21]. Executive function was derived from the Stroop Color Word Test (Part III) and a Verbal Fluency Test. Psychomotor speed was derived from the Line Tracing Test (LTT), Serial Dotting Test (SDT), and Number Connection Test type-A (NCT-A). Depression and anxiety were measured using the Self-Rating Depression Scale (SDS) and Self-Rating Anxiety Scale (SAS) [22, 23].

Blood and urine tests

All subjects underwent blood tests before MRI examinations, including total cholesterol (TC), triglycerides (Tri), high-density lipoprotein cholesterol (HDL-C), low-density lipoprotein cholesterol (LDL-C), fasting blood glucose (FBG), hemoglobin A1c (HbA1c), serum creatinine (Scr), blood uric acid (UA), blood urea nitrogen (BUN), cystatin C (Cyst), 24-h urine protein test was acquired in all patients.

MRI data acquisition

All MR imaging was performed on a 3.0-T scanner, equipped with a 12-channel head coil. For each subject, rs-fMRI data, DTI data, and high-resolution T1-weighted anatomic imaging data were acquired. The rs-fMRI scan lasted for 500 s and 250 brain volumes were collected. For rs-fMRI, all participants were instructed to stay awake, keep their head still, relax with their eyes closed, and not think of anything in particular. DTI data consisted of 20 volumes with diffusion gradients applied along 20 nonlinear directions ($b = 1000$ s/mm^2) and 1 volume without diffusion weighting ($b = 0$ s/mm^2). Each volume consisted of 30 contiguous axial slices. High-resolution T1-weighted images were acquired in the sagittal orientation with a magnetization-prepared rapid gradient echo sequence. Axial T2 fluid-attenuated inversion recovery sequence was also conducted to exclude clinically silent brain lesions. All the scanning parameters are consistent with our previous articles [24, 25]. For detailed imaging parameters, see Electronic supplementary material.

MRI data preprocessing

The rs-fMRI data were preprocessed using Data Processing Assistant for Resting-State fMRI (DPARSF) [26]. The preprocessing steps included removal of the first ten volumes, slice timing, realignment, regression of nuisance signals, spatial normalization, smoothing, and band-pass filtering. The DTI data were preprocessed using PANDA [27] with the following steps: converting DICOM files into NIfTI format, estimating the brain mask, cropping the raw images, coregistering to the b0 images, correcting for the eddy current distortions and head motions, tracking whole-brain fiber, averaging multiple directions, and calculating diffusion tensor metrics (details in the Electronic supplementary material).

Construction of brain networks

In this study, functional networks were obtained from rs-fMRI temporal series correlations, while structural networks were constructed using DTI tractography in all participants. The nodes of the functional and structural networks were delimited according to an automated anatomical labeling (AAL) algorithm [28]. This algorithm scheme divided the entire cerebral cortex (except the cerebellum) into 90 anatomical regions, which resulted in 90 nodes covering the noncerebellar brain and 45 nodes in each hemisphere (Fig. 1). The detailed construction steps are shown in the Electronic supplementary material.

Table 1 Demographics, clinical characteristics, and neuropsychological tests of all participants

Variables	DKD ($n = 62$)	DM ($n = 60$)	HC ($n = 80$)	p value
Demographic factors				
Age (years)	53 ± 9	52 ± 12	49 ± 13	0.199
Gender (M/F)	42/20	40/20	52/28	0.941[a]
Education (years)	9.76 ± 3.62	10.4 ± 3.66	10.86 ± 4.89	0.297
Duration of diabetes (years)	12.08 ± 4.78	7.78 ± 5.71	–	0.039[b]
Diabetic retinopathy (%)	40/62	30/60	–	0.143[a]
Diabetic peripheral neuropathy (%)	28/62	19/60	–	0.140[a]
Clinical variables				
BMI (kg/m^2)	24.96 ± 3.46	24.58 ± 3.27	24.05 ± 2.99	0.244
SBP (mm Hg)	147.1 ± 22.68	130.8 ± 14.19	124.71 ± 14.78	< 0.001
DBP (mm Hg)	82.52 ± 11.79	77.97 ± 8.90	73.83 ± 11.50	< 0.001
TC (mmol/L)	5.09 ± 1.59	4.59 ± 0.74	4.82 ± 0.84	0.060
Triglycerides (mmol/L)	1.78 ± 0.79	1.77 ± 1.28	1.32 ± 0.72	0.005
HDL-C (mmol/L)	0.91 ± 0.28	1.06 ± 0.24	1.29 ± 0.32	< 0.001
LDL-C (mmol/L)	2.82 ± 1.24	2.75 ± 0.66	2.78 ± 0.70	0.910
TIV (cm^3)	1480 ± 149.2	1504 ± 124.9	1515 ± 117.8	0.266
Fazekas scale score				
PV, 0/1/2/3	37/16/5/4	45/7/6/2	71/5/3/1	< 0.001[c]
DS, 0/1/2/3	22/32/3/5	31/23/4/2	54/18/6/2	0.003[c]
Diabetes-related characteristics				
FBG (mmol/L)	7.61 ± 2.62	7.60 ± 2.84	4.19 ± 0.87	< 0.001
HbA1c (mmol/mol)	62.88 ± 23.04	72.56 ± 24.22	35.20 ± 5.30	< 0.001
HbA1c (%)	7.90 ± 2.11	8.79 ± 2.22	5.37 ± 0.49	< 0.001
Kidney disease-related characteristics				
eGFR (mL/min/1.73 m^2)	48.61 ± 37.77	122.46 ± 38.98	109.12 ± 35.69	< 0.001
Scr (μmol/L)	216.2 ± 229.1	54.53 ± 15.62	60.14 ± 15.55	< 0.001
UA (μmol/L)	399.7 ± 111.3	322.9 ± 112.2	314.9 ± 72.4	< 0.001
BUN (mmol/L)	25.54 ± 23.80	12.30 ± 2.66	5.81 ± 1.26	< 0.001
Cyst C (mg/L)	1.86 ± 1.08	0.96 ± 0.22	0.95 ± 0.23	< 0.001
Urine protein (g/24 h)	4.71 ± 4.45	0.41 ± 0.47	–	< 0.001[b]
Neuropsychological score				
MMSE	27.74 ± 1.60	27.90 ± 1.41	28.70 ± 1.31	< 0.001
MoCA	22.45 ± 4.63	24.25 ± 2.85	26.59 ± 2.40	< 0.001
Immediate recall (n)	19.00 ± 4.16	20.18 ± 5.03	20.57 ± 5.94	0.303
Delay recall (n)	5.76 ± 1.73	6.39 ± 2.12	6.77 ± 2.13	0.040
Stroop I (s)	21.49 ± 4.88	19.83 ± 10.14	18.60 ± 7.94	0.231
Stroop II (s)	32.73 ± 8.31	27.84 ± 14.72	25.26 ± 8.84	0.006
DST (n)	31.83 ± 13.35	42.60 ± 14.14	53.40 ± 19.76	< 0.001
Stroop III (s)	41.49 ± 9.09	37.67 ± 16.05	31.48 ± 11.86	< 0.001
Verbal fluency (n)	3.68 ± 1.65	3.96 ± 1.72	4.87 ± 2.73	0.010
LTT (s)	84.05 ± 30.47	70.31 ± 32.78	46.84 ± 36.50	< 0.001
SDT (s)	49.54 ± 11.27	44.36 ± 16.95	42.58 ± 18.44	0.093
NCT-A (s)	69.90 ± 36.35	52.88 ± 42.35	50.98 ± 36.62	0.031
SAS	28.36 ± 5.55	27.22 ± 6.19	27.25 ± 5.71	0.492
SDS	27.74 ± 6.21	27.42 ± 6.58	26.49 ± 5.33	0.449

M = male; *F* = female; *BMI* = body mass index; *SBP* = systolic pressure; *DBP* = diastolic pressure; *TC* = total cholesterol; *HDL-C* = high-density lipoprotein cholesterol; *LDL-C* = low-density lipoprotein cholesterol; *TIV* = total intracranial volume; *PV* = periventricular; *DS* = deep subcortical; *FBG* = fasting blood glucose; *HbA1c* = hemoglobin A1c; *eGFR* = estimated glomerular filtration rate; *Scr* = serum creatinine; *UA* = urea acid; *BUN* = blood urea nitrogen; *Cyst C* = cystatin C; *MMSE* = Mini-Mental State Examination; *MoCA* = Montreal Cognitive Assessment; *DST* = Digit Symbol Test; *LTT* = Line Tracing Test; *SDT* = Serial Dotting Test; *NCT-A* = Number Connection Test type-A; *SAS* = Self-Rating Anxiety Scale; *SDS* = Self-Rating Depression Scale

[a] p value was calculated with the chi-square test

[b] p value was calculated with the two independent samples t test

[c] Fazekas scale was done using the Kruskal–Wallis test

Graph theory analysis

For the large-scale functional and structural networks, graph theoretical properties were calculated using the GRETNA toolbox [29]. We calculated the network topologic properties at the global level, which included (1) small-world parameters: clustering coefficient (Cp), characteristic path length (Lp), normalized clustering coefficient (γ), normalized characteristic path length (λ), and small-worldness (σ); and (2) network efficiency parameters: global efficiency (Eg) and local efficiency (Eloc). Supplementary Table 1 gives detailed descriptions of the abovementioned seven parameters.

When brain graphs were constructed, each graph of the subjects was thresholded to create an equal number of nodes and edges across subjects. We operated network parameters over a range of threshold values to guarantee high correlation coefficients of the remaining connections. We chose a sparsity threshold (range from 0.05 to 0.4 with an interval of 0.01) to convert each of the resulting correlation matrices into a series of weighted networks [30, 31]. We further calculated the area under the curve (AUC) over the sparsity for the between-group comparisons. The AUC provides a summarized scale for the topologic characterization of brain networks independent of a single threshold selection. This approach enabled the exploration of between-group differences in relative network organization, which is sensitive to topologic alterations in brain disorders [32].

Total intracranial volume analysis

Considering the potential effect of brain volume on functional and structural network changes, we analyzed the total intracranial volume (TIV) differences among the three groups. High-resolution T1-weighted anatomic images were processed in the SPM12 (Statistical Parametric Mapping12) toolbox (http://www.fil.ion.ucl.ac.uk/spm/software/spm12) to obtain TIV for each participant.

Functional–structural coupling analysis

For each subject, we calculated the Pearson correlation coefficients between functional and structural network matrix, which is considered as network coupling value. The detailed calculation steps are shown in the Electronic supplementary material.

White matter lesions and image quality

Considering that that cerebral white matter lesions (WML) play a role in cognitive decline, we used the Fazekas scale to quantify WML burden, which include periventricular (PV) scores and deep subcortical (DS) scores [33, 34]. Two experienced neuroradiologists evaluated and verified image quality, presence of obvious brain lesions, and Fazekas scale for each subject.

Subgroup analysis in DKD patients

To further explore whether the decreased estimated glomerular filtration rate (eGFR) had an adverse effect on the brain network alterations, we divided the DKD patient groups into two subgroups: CKD1–3 group (which was defined as eGFR ≥ 60 mL/min/1.73 m^2) consisting of 45 patients (CKD stage 1, $n = 15$; CKD stage 2, $n = 11$; and CKD stage 3, $n = 19$) and CKD4–5 group (which was defined as eGFR < 60 mL/min/1.73m^2) consisting of 17 patients (CKD stage 4, $n = 7$; and CKD stage 5, $n = 10$). Detailed information for these DKD patients is summarized in Supplementary Table 2.

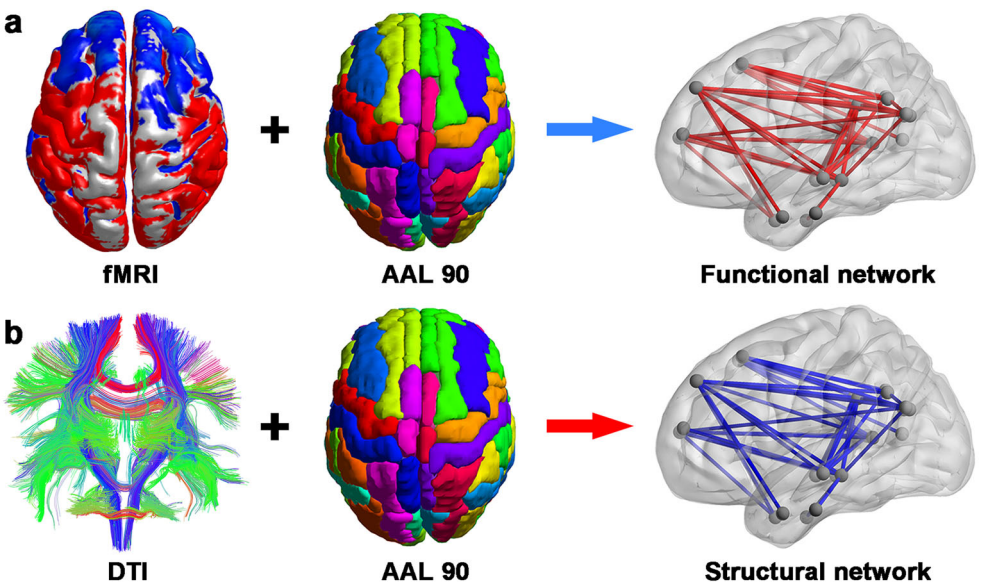

Fig. 1 **a**, **b** Flowchart of fMRI-based functional network and DTI-based structural network construction. In this study, functional networks were obtained from rs-fMRI temporal series correlations, while structural networks were constructed using DTI tractography in all participants. The nodes of the functional and structural networks were delimited according to an automated anatomical labeling (AAL) algorithm

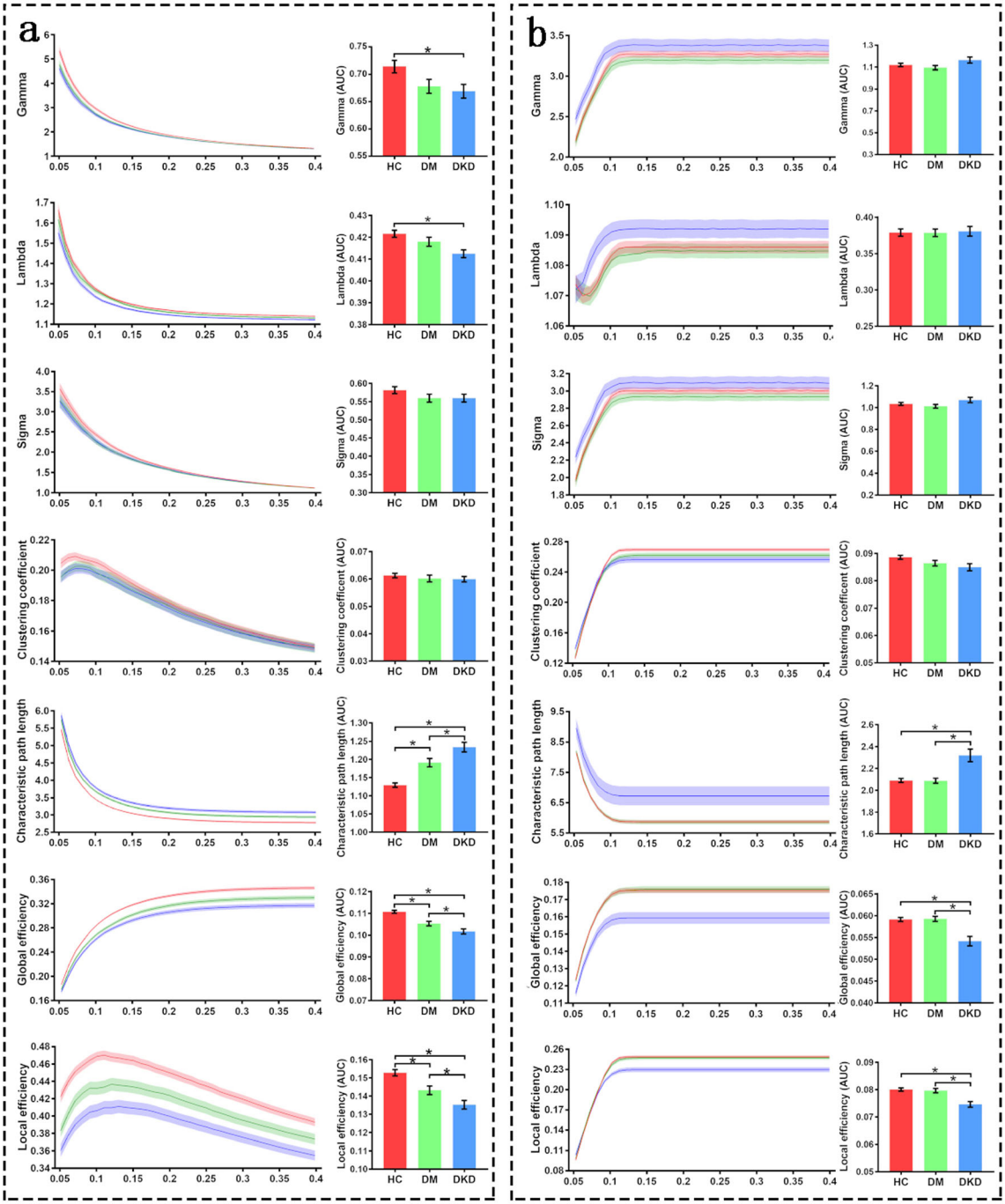

Fig. 2 Functional and structural networks in all three groups. Functional (**a**) and structural (**b**) network measures of the global organization of the brain for healthy controls (red), DM patients (green), and DKD patients (blue). The left column represents the results from a range of sparsity values (0.05–0.4). Straight lines indicate the mean values of the groups, and the corresponding transparent areas represent the standard error of the mean. The right column represents the results from area under the curve (AUC) values. * indicates significant group differences after post hoc pairwise comparisons ($p < 0.05$ after Bonferroni-corrected)

Statistical analysis

Statistical analysis of demographic, neuropsychological, and clinical data was performed using SPSS software. Group differences were tested using analysis of covariance (ANCOVA) for quantitative variables and chi-square tests for qualitative variables, if appropriate. Post hoc analysis was performed if the ANCOVA test showed significant differences. We further studied the differences of graph theory parameters between the CKD1–3 group and the CKD4–5 group using an independent two-samples *t* test. After significant intergroup differences were identified in the network measures, Pearson

Table 2 Brain network graph measures in participants of the three groups

Graph measures	DKD ($n = 62$)	DM ($n = 60$)	HC ($n = 80$)	p value
Functional network				
Gamma	0.669 ± 0.099	0.678 ± 0.098	0.714 ± 0.100	0.009
Lambda	0.412 ± 0.014	0.418 ± 0.016	0.422 ± 0.014	0.039
Sigma	0.559 ± 0.085	0.559 ± 0.086	0.581 ± 0.086	0.085
Cp	0.060 ± 0.008	0.060 ± 0.010	0.061 ± 0.007	0.717
Lp	1.234 ± 0.105	1.191 ± 0.088	1.129 ± 0.053	< 0.001
Eg	0.102 ± 0.009	0.105 ± 0.008	0.111 ± 0.006	< 0.001
Eloc	0.135 ± 0.019	0.143 ± 0.018	0.153 ± 0.016	< 0.001
Structural network				
Gamma	1.165 ± 0.220	1.096 ± 0.147	1.120 ± 0.137	0.091
Lambda	0.381 ± 0.007	0.378 ± 0.005	0.379 ± 0.005	0.078
Sigma	1.070 ± 0.195	1.012 ± 0.130	1.034 ± 0.120	0.121
Cp	0.085 ± 0.010	0.086 ± 0.008	0.089 ± 0.007	0.134
Lp	2.320 ± 0.457	2.088 ± 0.178	2.091 ± 0.168	0.001
Eg	0.054 ± 0.009	0.059 ± 0.004	0.059 ± 0.004	< 0.001
Eloc	0.075 ± 0.008	0.080 ± 0.006	0.080 ± 0.005	0.001
Functional–structural coupling				
Coupling	0.479 ± 0.058	0.448 ± 0.056	0.472 ± 0.052	0.005

Graph measures of functional and structural network are area under the curve (AUC) of the network properties across the full range of sparsity thresholds

Cp = clustering coefficient; *Lp* = characteristic path length; *Eg* = global efficiency; *Eloc* = local efficiency

correlations were computed to examine the relationships between these measures and the neuropsychological and clinical data in type 2 diabetes patients. The potential confounding factors including age, sex, education levels, TIV, disease duration, Fazekas score, and emotional scale scores were set as nuisance covariates in these analyses. A p value < 0.05 was considered as statistically different.

Results

Demographics and clinical and neuropsychological data

There were no differences in age, sex, or educational level among the three groups (all $p > 0.05$). The groups had different laboratory indexes which are related to diabetes and kidney disease. The patient groups scored lower than the healthy control subjects in the MMSE and MoCA tests (all $p < 0.05$). DKD patients performed worse in the delay memory function test compared with HCs ($p < 0.05$). DKD patients performed worse than the controls in the Stroop II test ($p < 0.05$). The DST score differed significantly among the three groups (all $p < 0.05$). DKD patients performed worse than the controls in the Stroop III test and the Verbal Fluency Test (all $p < 0.05$). DKD and DM patients performed worse than the controls in the LCT and NCT-A (all $p < 0.05$). The demographic and clinical details of all participants are summarized in Table 1.

Functional and structural network analysis

Small-worldness properties

All three groups demonstrated economical small-world organization (γ larger than 1 and λ close to 1) [35] in the functional and structural networks. We noticed significantly decreased γ and λ in the functional network rather than in the structural network in DKD patients. Moreover, DKD patients manifested lower Lp than the other two groups in both functional and structural networks. The Lp of DM patients fell between those of the DKD and controls in the functional network (all $p < 0.05$, Bonferroni-corrected) (Fig. 2a, b and Table 2).

Network efficiency analysis

For the functional network efficiency, DKD patients displayed lower Eg and Eloc values compared with controls, while DM patients showed intermediate values between those two groups (Fig. 2a and Table 2) (all $p < 0.05$ after Bonferroni-corrected). For the structural network efficiency, DKD patients also showed decreased Eg and Eloc compared with DM patients and controls (all $p < 0.05$ after Bonferroni-corrected); however, no differences for Eg and Eloc were found between DM patients and controls (Fig. 2b and Table 2).

Functional–structural coupling analysis results

DM patients showed decreased functional–structural coupling compared with controls and DKD patients (both $p < 0.05$ after Bonferroni-corrected). However, there were no differences between DKD patients and controls (Fig. 3 and Table 2).

Different CKD stage analysis results

In the functional network, the CKD4–5 group performed worse in nearly all parameters (except for γ, $p = 0.07$) than the CKD1–3 group. In the structural network, only Lp and Eg were influenced in the CKD4–5 group compared with the CKD1–3 group (all $p < 0.05$) (Fig. 4). No differences were found for functional–structural coupling between the two subgroups.

Correlation results

We performed correlation analysis between global-level network parameters and clinical data results with statistical difference in the ANCOVA test. BUN, eGFR, and UA were the first three clinical blood biochemical variables correlating with Lp, Eg, and Eloc in the structural networks (Fig. 5a, Supplementary Table 3). The diabetes duration was correlated with aLp and aEg ($r = 0.354$, $p < 0.001$; $r = -0.323$, $p < 0.001$, respectively) in the functional network and aEloc ($r = -0.302$, $p < 0.001$) in the structural network.

The same phenomenon was also observed in the correlation analysis between global-level network parameters and neuropsychological test results. In the structural network, Lp positively correlated with information processing speed (Stroop II, $r = 0.316$, $p = 0.002$), Eg and Eloc were associated with information processing speed (with Stroop II, $r = -0.348$ and -0.383, respectively, both $p < 0.001$; with DST, $r = 0.335$, $p = 0.001$; $r = 0.386$, $p < 0.001$,respectively), while Eg and Eloc negatively associated with psychomotor speed (LTT, $r = -0.334$, $r = -0.342$, both $p = 0.001$) (Fig. 5b, Supplementary Table 3). No correlations were found for any other parameters between global-level network parameters of the functional network and neuropsychological results except for the λ and DST ($r = 0.338$, $p = 0.001$).

Discussion

This study found that DKD patients showed disrupted functional and structural brain networks compared with DM patients and healthy controls, which was especially apparent in functional and structural brain network efficiency measures. Reduced kidney function clearly deteriorated functional and structural brain networks. We also found that structural network efficiency rather than functional network efficiency was correlated with BUN and cognitive performance.

We found that the functional and structural brain networks in all three groups were characteristic of small-world properties [36]. However, lower γ and λ values in DKD patients hint functional network shifts toward "randomization" in DKD rather than DM patients. Network "randomization" means decreased local specialization and global integration. It has also been observed in other neuropsychiatric disorders such as major depressive disorder, schizophrenia, and Alzheimer's disease [32, 37, 38]. Importantly, we found that changes of functional and structural network topological properties were asynchronous. Our findings are consistent with two previous studies

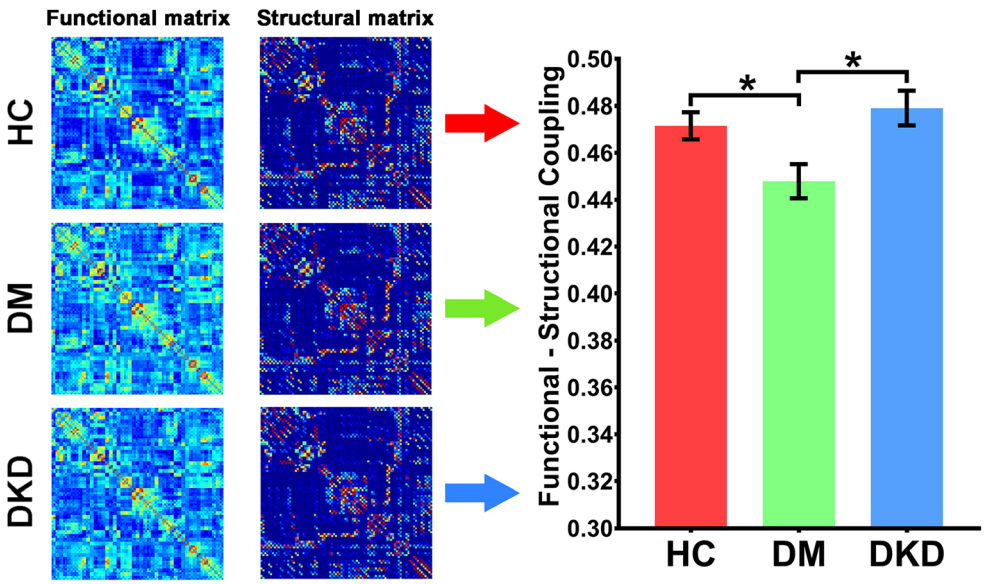

Fig. 3 Functional and structural network coupling of all three groups. The average functional–structural connectivity coupling of the two patient groups and healthy controls. The DM patients show decreased functional–structural coupling compared with healthy controls and DKD patients (both $p < 0.05$ after Bonferroni-corrected). However, there are no differences between DKD patients and healthy controls

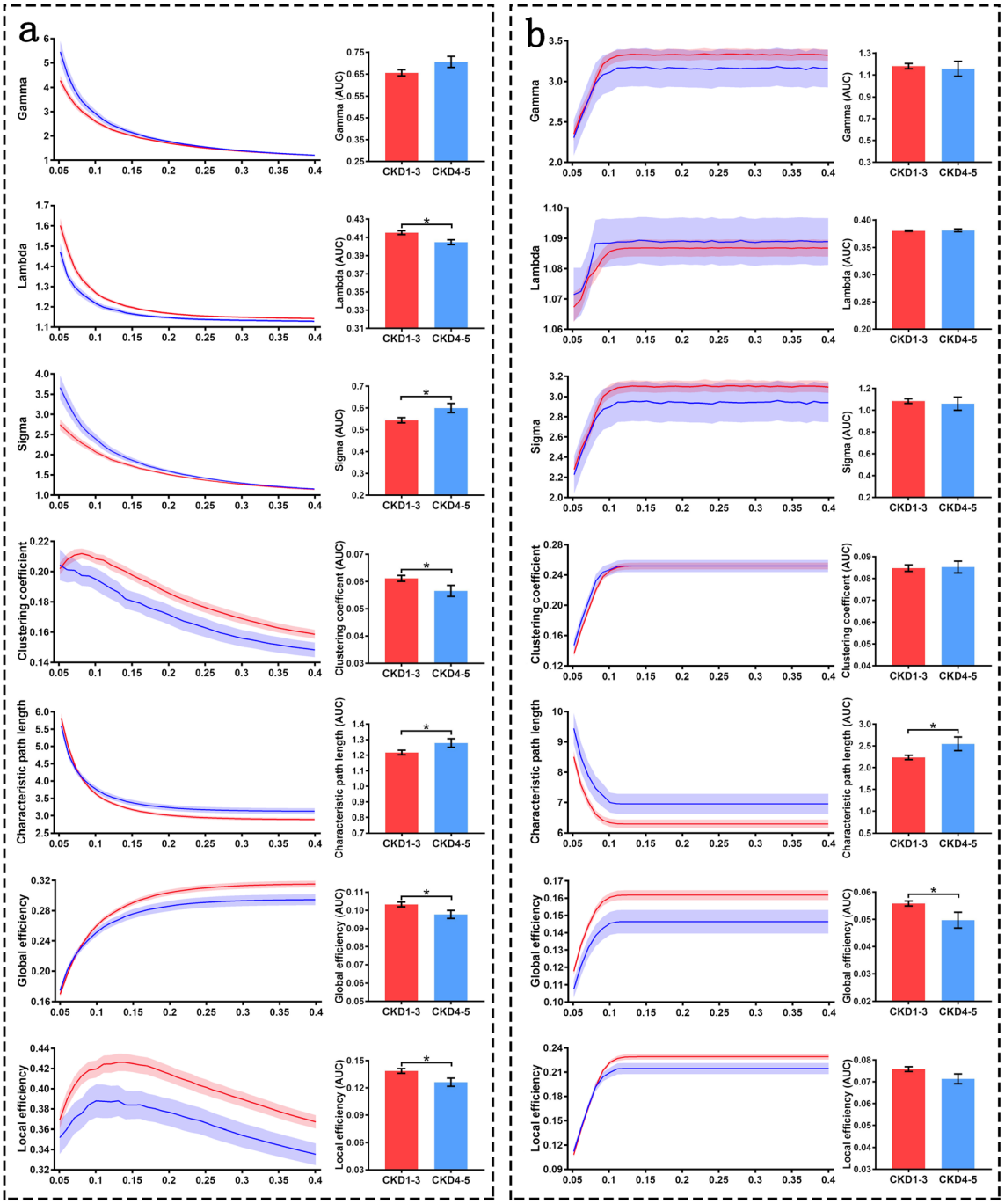

Fig. 4 Functional and structural networks in DKD patients with different CKD stages. Functional (**a**) and structural (**b**) network measures of the global organization of the brain for DKD patients with CKD1–3 (red) and CKD4–5 (blue). The left column represents the results from a range of sparsity values (0.05–0.4). Straight lines indicate the mean values of the groups, and the corresponding transparent areas represent the standard error of the mean. The right column represents the results from area under the curve (AUC) values. * indicates significant group differences ($p < 0.05$)

which found disrupted topological organization of the white matter network in type 2 diabetes patients [7, 39]. However, these two studies did not consider the effect of DKD on the brain structural topological properties. High prevalence of DKD in type 2 diabetes patients, especially the ones with long disease duration, has been reported. The UK National Diabetes Audit revealed that 63.7% type 2 diabetes patients had an eGFR < 60 mL/min/1.73 m^2 [40], while > 40% type 2 diabetes patients have DKD in the USA [41]. When diabetes duration exceeds 7–10 years, a clinical diagnosis of DKD should be considered [42]. In fact, long disease duration was reported in the studies of

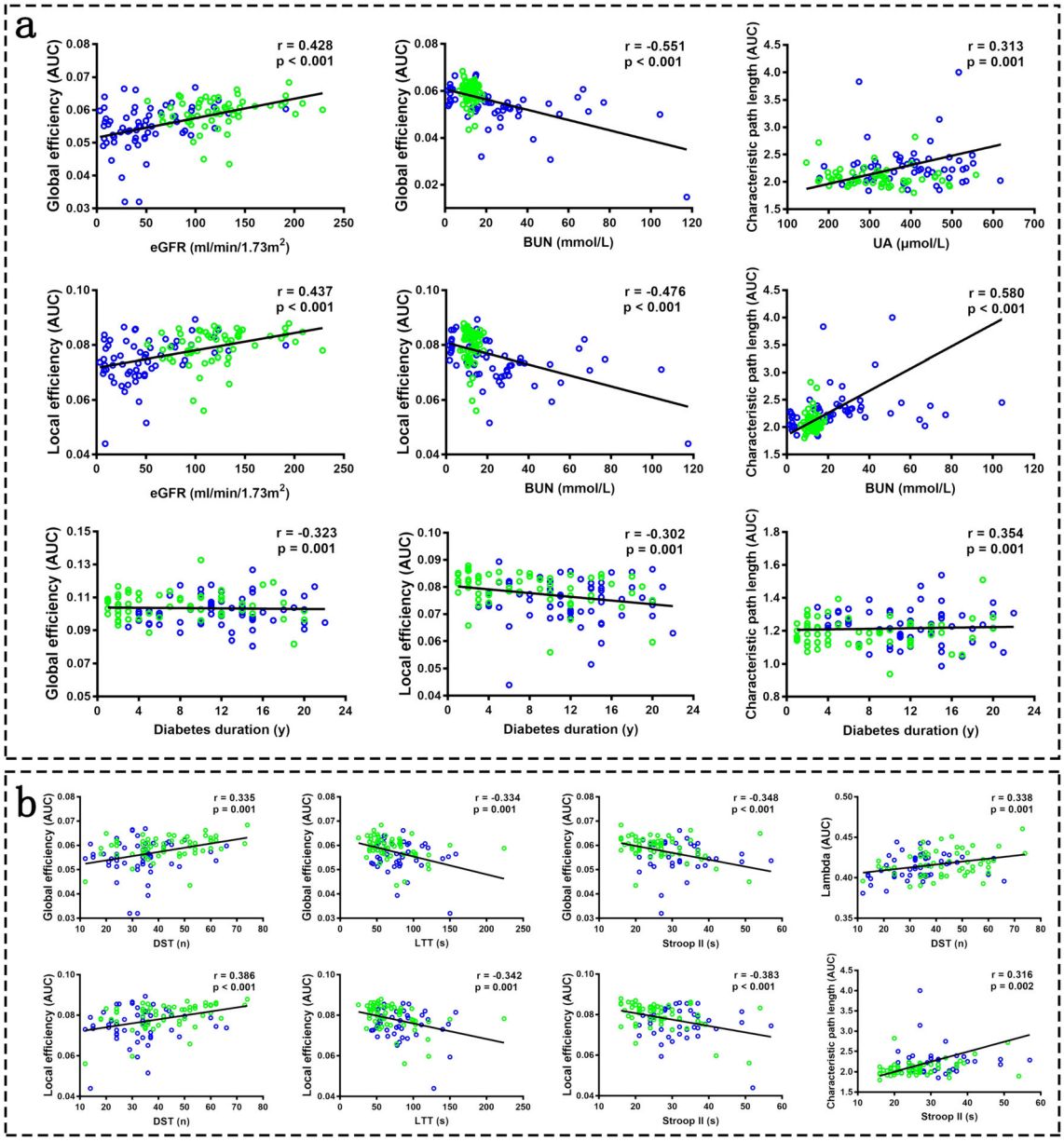

Fig. 5 Correlation analysis results between functional and structural network parameters and clinical and neuropsychological tests. **a** The correlation analysis results between functional and structural network parameters and clinical data. **b** The correlation analysis results between functional and structural network parameters and neuropsychological tests. Global efficiency and characteristic path length (**a**) (in the third row) and Lambda (**b**) belong to the functional network and the other network parameters belong to the structural network. The blue circle represents the DKD patient and the green circle represents the DM patient. AUC = area under the curve; eGFR = estimated glomerular filtration rate; BUN = blood urea nitrogen; UA = urea; DST = Digit Symbol Test; LTT = Line Tracing Test

Reijmer et al (8 (1–51) years) and Zhang et al (6.1 ± 3.1 years), respectively. The DKD subgroups analysis indicated that impaired kidney function did have a negative effect on large-scale functional and structural networks. It is possible that renal toxins such as BUN and UA may play a role in disrupting structural network in DKD patients, resulting in abnormal functional network [43–45]. Taken together, these findings indicate that functional network reorganization progressively emerges but the structural network remains intact in type 2 diabetes patients without kidney complications, which are further aggravated as kidney function declines in DKD patients (Fig. 6).

One interesting phenomenon was that DKD patients displayed normally appearing functional–structural coupling compared with DM patients, which can be attributed to both disrupted functional and structural connectivity in DKD patients (Fig. 6). Our study found functional–structural decoupling in DM patients compared with controls, which has not been reported in DM patients. However, some previous studies have found functional–structural decoupling in

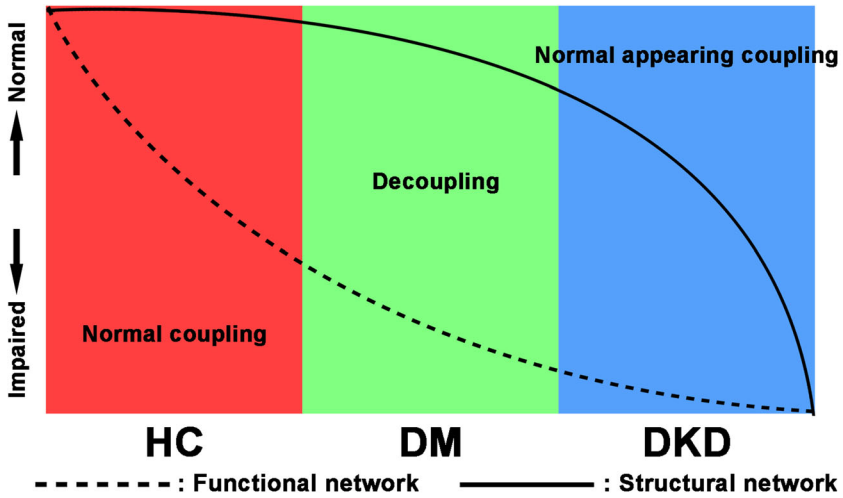

Fig. 6 Hypothetical overview of functional and structural network reorganization as the disease progresses. Before the onset of diabetes mellitus (DM), the functional and structural cerebral networks showed normal organization as well as normal coupling. When in the DM stage, the functional network is firstly affected and begins to fall, while the structural network still remains largely intact compared with the controls. The different network alterations in this stage thus lead to functional–structural decoupling. Finally, when DM progresses to diabetic kidney disease (DKD), both the functional network and the structural network are disrupted in this stage, which may lead to "normally appearing" functional–structural coupling. The red, green, and blue areas indicate the healthy, DM, and DKD stages, respectively. The dashed line represents the functional network and the full line represents the structural network

epilepsy, which suggested that the functional–structural decoupling may reflect the progress of long-term cognitive impairment in epilepsy [46]. Furthermore, we did not find significant differences in functional–structural coupling between the two subgroups in DKD patients, which can be attributed to small sample size and other confounding factors such as age and dialysis duration. This also indicated that functional–structural coupling may not be an optimal imaging biomarker for revealing the disease progression in DKD patients.

We found that there were weak correlations between structural network properties and patients' neuropsychological results, and information processing speed and psychomotor speed were preferentially affected in patients with diabetes. These findings have been reported in one previous study in type 2 diabetes patients [7]. Reijmer et al reported that local and global network properties (i.e., Cp, Eg, Lp) were altered and associated with impaired processing speed [7]. However, in our study, no functional network parameters except for λ were found to be correlated with neuropsychological test results. We speculate the possible cause is that functional connectivity is more flexible than structural connectivity. Further studies are needed to clarify this issue.

Our study has some limitations. The cross-sectional design limited our ability to demonstrate how functional and structural brain networks dynamically reorganize as DM progresses to DKD. Future longitudinal studies are needed. For graph-based brain network studies, node definition and selection are very important in building structural or functional brain networks. However, there is still controversy regarding the optimal analytic strategies [47]. Future studies could choose nodes according to different brain anatomical or functional templates offering insight at reduced spatial scales. There remain many clinical factors, such as diabetes medication (e.g., oral hypoglycemic drugs, injection of insulin, or CKD-related treatments) and other nonrenal complications (such as diabetic retinopathy and diabetic peripheral neuropathy), that have the potential effects on our study results However, it is rather difficult to avoid these factors because the treatments have to be administrated to prevent the deterioration of the diseases.

In conclusion, this study demonstrates that DKD is associated with progressive functional and structural network disorganization of the brain connectome and normally appearing functional–structural coupling compared with type 2 diabetes patients without kidney complications, which can be further aggravated as kidney function declines. This provides an implicative neural basis for the alterations of brain networks in DKD patients and highlights the role of the kidney–brain axis in neurocognitive dysfunction.

Funding This study was funded by grants from the National Natural Science Foundation of China (81322020, 81230032, 81471644).

Compliance with ethical standards

Guarantor The scientific guarantor of this publication is Long Jiang Zhang.

Conflict of interest The authors declare that they have no conflicts of interest.

Statistics and biometry No complex statistical methods were necessary for this paper.

Informed consent Written informed consent was obtained from all subjects (patients) in this study.

Ethical approval Institutional Review Board approval was obtained.

Study subjects or cohorts overlap Some study subjects or cohorts have not been previously reported.

Methodology
- prospective
- observational
- performed at one institution

References

1. Ingelfinger JR, Jarcho JA (2017) Increase in the incidence of diabetes and its implications. N Engl J Med 376:1473–1474
2. Polonsky KS (2012) The past 200 years in diabetes. N Engl J Med 367:1332–1340
3. Yang W, Lu J, Weng J et al (2010) Prevalence of diabetes among men and women in China. N Engl J Med 362:1090–1101
4. Gregg EW, Li Y, Wang J et al (2014) Changes in diabetes-related complications in the United States, 1990-2010. N Engl J Med 370: 1514–1523
5. [No authors listed] (2015) Diabetic kidney disease: what does the next era hold? Lancet Diabetes Endocrinol 3:665
6. de Boer IH (2017) A new chapter for diabetic kidney disease. N Engl J Med 377:885–887
7. Reijmer YD, Leemans A, Brundel M, Kappelle LJ, Biessels GJ, Utrecht Vascular Cognitive Impairment Study Group (2013) Disruption of the cerebral white matter network is related to slowing of information processing speed in patients with type 2 diabetes. Diabetes 62:2112–2115
8. van Bussel FC, Backes WH, van Veenendaal TM et al (2016) Functional brain networks are altered in type 2 diabetes and prediabetes: signs for compensation of cognitive decrements? The Maastricht study. Diabetes 65:2404–2413
9. Sink KM, Divers J, Whitlow CT et al (2015) Cerebral structural changes in diabetic kidney disease: African American-Diabetes Heart Study MIND. Diabetes Care 38:206–212
10. Murea M, Hsu FC, Cox AJ et al (2015) Structural and functional assessment of the brain in European Americans with mild-to-moderate kidney disease: Diabetes Heart Study-MIND. Nephrol Dial Transplant 30:1322–1329
11. Bressler SL, Menon V (2010) Large-scale brain networks in cognition: emerging methods and principles. Trends Cogn Sci 14:277–290
12. Bullmore E, Sporns O (2009) Complex brain networks: graph theoretical analysis of structural and functional systems. Nat Rev Neurosci 10:186–198
13. Bullmore E, Sporns O (2012) The economy of brain network organization. Nat Rev Neurosci 13:336–349
14. Vaessen MJ, Jansen JF, Vlooswijk MC et al (2012) White matter network abnormalities are associated with cognitive decline in chronic epilepsy. Cereb Cortex 22:2139–2147
15. Bassett DS, Bullmore ET (2009) Human brain networks in health and disease. Curr Opin Neurol 22:340–347
16. Zheng G, Wen J, Zhang L et al (2014) Altered brain functional connectivity in hemodialysis patients with end-stage renal disease: a resting-state functional MR imaging study. Metab Brain Dis 29: 777–786
17. Zhang LJ, Zheng G, Zhang L et al (2012) Altered brain functional connectivity in patients with cirrhosis and minimal hepatic encephalopathy: a functional MR imaging study. Radiology 265:528–536
18. Zhang LJ, Zheng G, Zhang L et al (2014) Disrupted small world networks in patients without overt hepatic encephalopathy: a resting state fMRI study. Eur J Radiol 83:1890–1899
19. American Diabetes Association (2018) 2. Classification and diagnosis of diabetes: standards of medical care in diabetes—2018. Diabetes Care 41:S13–S27
20. KDOQI (2007) KDOQI clinical practice guidelines and clinical practice recommendations for diabetes and chronic kidney disease. Am J Kidney Dis 49:S12–S154
21. Van der Elst W, Van Boxtel MP, Van Breukelen GJ, Jolles J (2006) The Stroop color-word test: influence of age, sex, and education; and normative data for a large sample across the adult age range. Assessment 13:62–79
22. Zung WW (1971) A rating instrument for anxiety disorders. Psychosomatics 12:371–379
23. Faravelli C, Albanesi G, Poli E (1986) Assessment of depression: a comparison of rating scales. J Affect Disord 11:245–253
24. Wang YF, Kong X, Lu GM, Zhang LJ (2017) Diabetes mellitus is associated with more severe brain spontaneous activity impairment and gray matter loss in patients with cirrhosis. Sci Rep 7:7775
25. Zhang LJ, Wen J, Liang X et al (2016) Brain default mode network changes after renal transplantation: a diffusion-tensor imaging and resting-state functional MR imaging study. Radiology 278:485–495
26. Chao-Gan Y, Yu-Feng Z (2010) DPARSF: a MATLAB toolbox for "pipeline" data analysis of resting-state fMRI. Front Syst Neurosci 4:13
27. Cui Z, Zhong S, Xu P, He Y, Gong G (2013) PANDA: a pipeline toolbox for analyzing brain diffusion images. Front Hum Neurosci 7:42
28. Tzourio-Mazoyer N, Landeau B, Papathanassiou D et al (2002) Automated anatomical labeling of activations in SPM using a macroscopic anatomical parcellation of the MNI MRI single-subject brain. Neuroimage 15:273–289
29. Wang J, Wang X, Xia M, Liao X, Evans A, He Y (2015) GRETNA: a graph theoretical network analysis toolbox for imaging connectomics. Front Hum Neurosci 9:386
30. Fornito A, Zalesky A, Bullmore ET (2010) Network scaling effects in graph analytic studies of human resting-state fMRI data. Front Syst Neurosci 4:22
31. Braun U, Plichta MM, Esslinger C et al (2012) Test-retest reliability of resting-state connectivity network characteristics using fMRI and graph theoretical measures. Neuroimage 59:1404–1412
32. Zhang J, Wang J, Wu Q et al (2011) Disrupted brain connectivity networks in drug-naive, first-episode major depressive disorder. Biol Psychiatry 70:334–342
33. Fazekas F, Chawluk JB, Alavi A et al (1987) MR signal abnormalities at 1.5 T in Alzheimer's dementia and normal aging. AJR Am J Roentgenol 149:351–356
34. Bournonville C, Hénon H, Dondaine T et al (2018) Identification of a specific functional network altered in poststroke cognitive impairment. Neurology 90:e1879–e1888
35. Watts DJ, Strogatz SH (1998) Collective dynamics of 'small-world' networks. Nature 393:440–442
36. Sporns O, Chialvo DR, Kaiser M, Hilgetag CC (2004) Organization, development and function of complex brain networks. Trends Cogn Sci 8:418–425
37. Lynall ME, Bassett DS, Kerwin R et al (2010) Functional connectivity and brain networks in schizophrenia. J Neurosci 30:9477–9487
38. Sanz-Arigita EJ, Schoonheim MM, Damoiseaux JS et al (2010) Loss of 'small-world' networks in Alzheimer's disease: graph

analysis of FMRI resting-state functional connectivity. PLoS One 5: e13788
39. Zhang J, Liu Z, Li Z et al (2016) Disrupted white matter network and cognitive decline in type 2 diabetes patients. J Alzheimers Dis 53:185–195
40. Hill CJ, Cardwell CR, Patterson CC et al (2014) Chronic kidney disease and diabetes in the National Health Service: a cross-sectional survey of the U.K. National Diabetes Audit. Diabet Med 31:448–454
41. Doshi SM, Friedman AN (2017) Diagnosis and management of type 2 diabetic kidney disease. Clin J Am Soc Nephrol 12:1366–1373
42. Tong L, Adler SG (2018) Diabetic kidney disease. Clin J Am Soc Nephrol 13:335–338
43. Luo S, Qi RF, Wen JQ et al (2016) Abnormal intrinsic brain activity patterns in patients with end-stage renal disease undergoing peritoneal dialysis: a resting-state functional MR imaging study. Radiology 278(1):181–189
44. Kong X, Wen JQ, Qi RF et al (2014) Diffuse interstitial brain edema in patients with end-stage renal disease undergoing hemodialysis: a tract-based spatial statistics study. Medicine (Baltimore) 93:e313
45. Bugnicourt JM, Godefroy O, Chillon JM, Choukroun G, Massy ZA (2013) Cognitive disorders and dementia in CKD: the neglected kidney-brain axis. J Am Soc Nephrol 24:353–363
46. Zhang Z, Liao W, Chen H et al (2011) Altered functional–structural coupling of large-scale brain networks in idiopathic generalized epilepsy. Brain 134:2912–2928
47. Zalesky A, Fornito A, Harding IH et al (2010) Whole-brain anatomical networks: does the choice of nodes matter. Neuroimage 50: 970–983